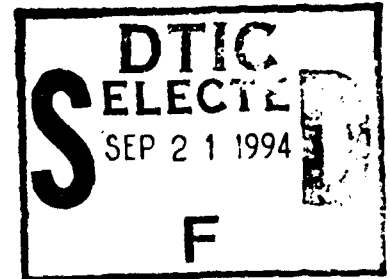AD-A284 796

‖‖‖‖‖‖‖‖‖‖‖‖

Quarterly Progress Report

June 1, 1994 to August, 31, 1994

Visible Light Emitting Materials and Injection Devices

ONR/ARPA URI

Grant Number N00014-92-J-1895

Prepared by:

Paul H. Holloway
Department of Materials Science and Engineering
University of Florida
P.O. Box 116400
Gainesville, FL 32611
Ph: 904/392-6664; FAX: 904/392-4911
E-Mail: Internet-PHOLL@MSE.UFL.EDU

Participants:
University of Florida
Kevin Jones
Robert Park
Joe Simmons
Dept. of Materials Science and Engineering
Tim Anderson
Dept. of Chemical Engineering
Peter Zory
Dept. of Electrical Engineering
University of Colorado
Jacques Pankove
Dept. of Electrical Engineering
Columbia University
Gertrude Neumark
Dept. of Materials Science and Engineering
Oregon Graduate Institute of Science and Engineering
Reinhart Engelmann
Dept. of Electrical Engineering

94-30177

‖‖‖‖‖‖‖‖‖‖‖‖

(I) Molecular Beam Epitaxy Growth of II-VI and III-Nitrides (Robert Park)

(a) Widegap II-VI Work

We completed an extensive investigation this quarter into the influence of growth parameters (including dopant source condition) on the free-hole concentration in p-type ZnSe:N epilayers which involved real-time *in situ* cathodoluminescence intensity measurements during growth as well as *ex situ* Hall-effect measurements on a number of selected samples. The parameters varied included nitrogen plasma integrated intensity, substrate temperature and II/VI beam equivalent pressure ratio.

CL intensity measurements were made *in situ* during epilayer growth using the apparatus illustrated in Fig. I.1. These measurements could be made in real-time as the various growth parameters were modified. In addition, free-hole concentrations were measured in films grown under particular conditions using the sample configuration illustrated in Fig. I.2. The ohmic contact mesas were deposited *in situ* through a mechanical mask which was introduced over the sample following the growth of the p-doped epilayer.

The data obtained from this study is being incorporated into a paper to be submitted shortly to the Journal of Applied Physics. Briefly, though, a strong correlation was found between the hole concentration measured *ex situ* at room temperature and the CL intensity monitored during epilayer growth. We believe, consequently, that this real-time measurement technique could be extremely useful in terms of process monitoring and control as well as for optimization of growth conditions for doping ZnSe and related materials.

(b) Column III-Nitride work.

Work in the nitride area was severely hampered this quarter due to the development of a leak in the MBE growth chamber. The leak was eventually determined to be associated with an electrical feedthrough on the nitrogen plasma source. The plasma source was returned to Oxford Applied Research in the U. K. in order that the feedthrough could be replaced which led to a rather lengthy delay. Prior to the leak problem, we had performed some preliminary studies of InGaN growth with a view, primarily, to establishing an optimum growth temperature regime for the alloy. The preliminary work was done on Si substrates in the interest of economy. However, we plan to grow the cubic phase, on β-SiC coated Si substrates when more is known about deposition parameters.

(II) Ohmic Contact Formation (Paul Holloway)

(a) ZnSe Contacts

Efforts have focused on Au and Ag contacts to p-type ZnSe. Previous work indicated that Ag produced contacts with a minimum Schottky barrier height of ~2.3 eV following heat treatment at 150°C for 45 minutes. In contrast, Au contacts were found to have a minimum barrier height of ~3 volts following heat treatment at 350°C for 30 to 45 minutes. The lower minimum barrier height of the Ag contacts was unexpected since Au has a larger

N₂

RF coil

phosphor
screen

PBN
discharge tube

Selenium

N
radicals

e-

UHV

ion
gauge

CCD video
camera

ΣSe

Cathodoluminescence

GaAs
substrate

Zn

Zinc

Te

p-ZnSe
epilayer

Tellurium

electron
gun
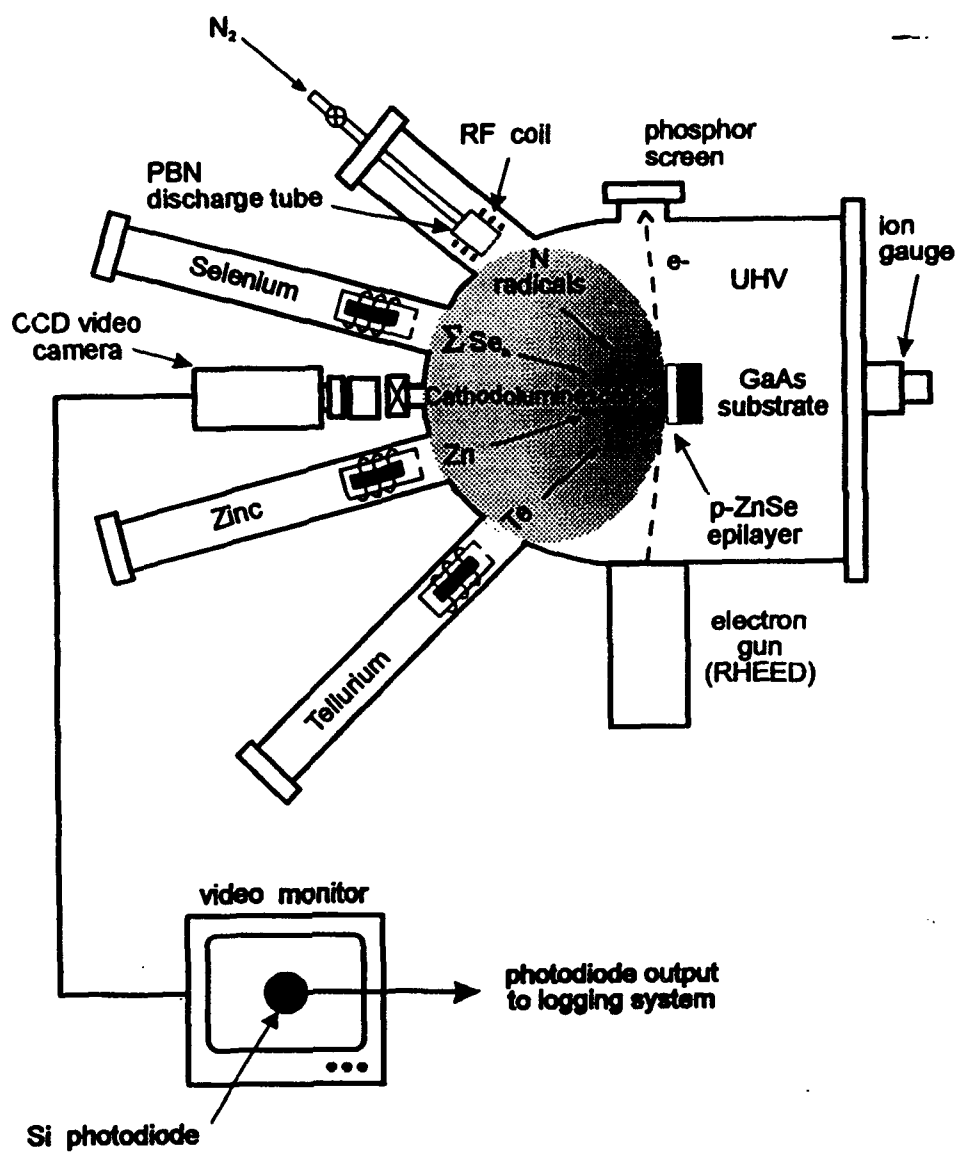(RHEED)

video monitor

photodiode output
to logging system

Si photodiode

Fig. I.1.   Schematic of ZnSe MBE growth chamber with detector system for *in situ*,
real-time monitoring of cathodoluminescence.

Te metallization

SPS p-ZnTe wells (numbers at left indicate well widths in Å)

SPS p-ZnSe barriers (each 20 Å wide)

17

11

8

6

5

4

3

p-ZnSe

Ohmic contact mesa detail
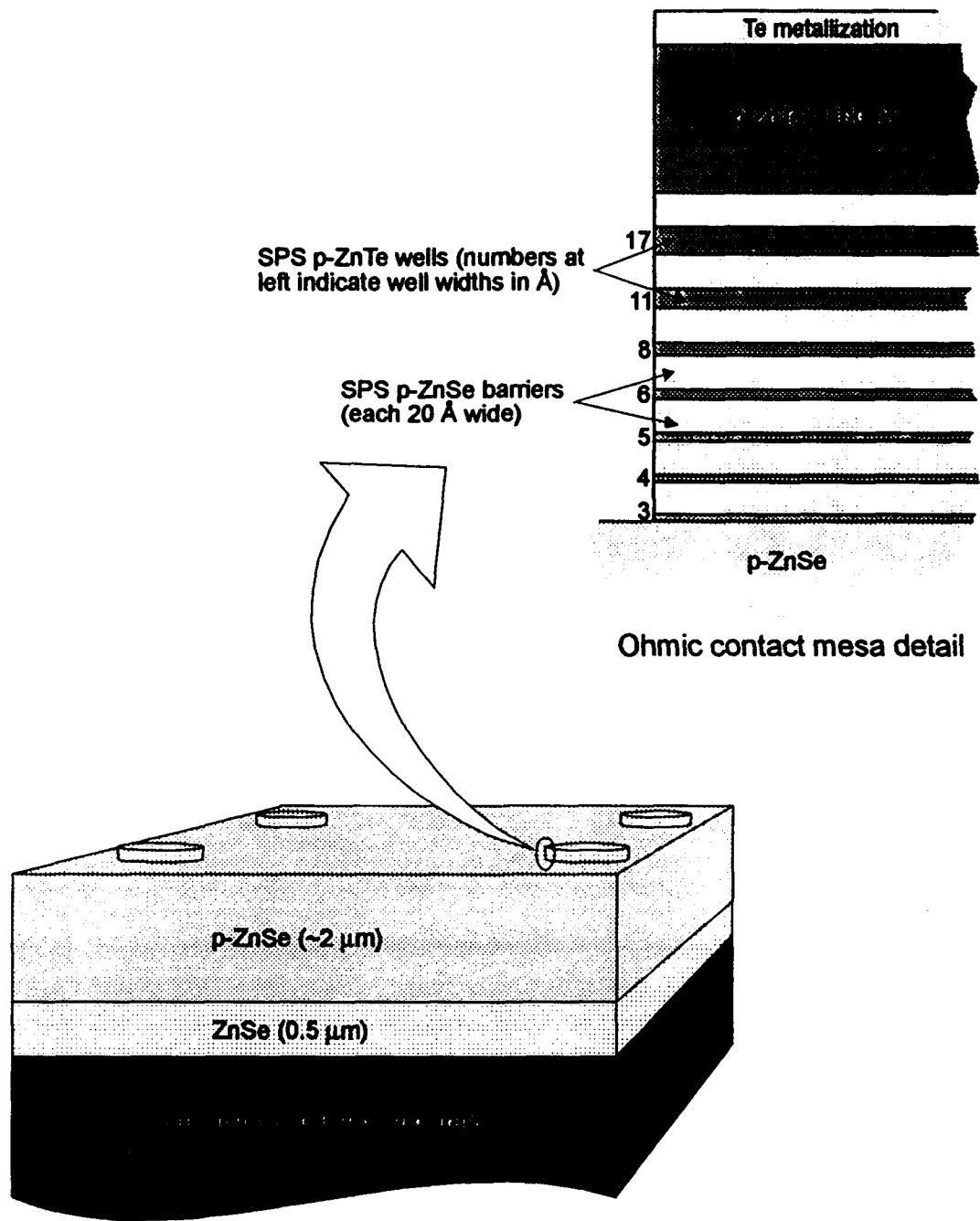
p-ZnSe (~2 µm)

ZnSe (0.5 µm)

Fig. I.2.   Schematic of sample for Hall measurements showing short-period superlattice (SPS) ohmic contact mesas formed by employing a shadow mask during the final stages of growth.

work function than Ag. Based on analytical results, the lower barrier height of the Ag contacts was attributed to the presence of oxygen (O) at the Ag/ZnSe interface.

A careful review has been performed to identify the mechanism(s) by which interfacial O may be reducing the Schottky barrier height of the Ag/ZnSe contacts. This survey indicated two possible mechanisms. First, O has been identified as a shallow p-type dopant in ZnSe with an ionization energy of ⁻80 meV. This indicates that interfacial O may be doping the surface of the ZnSe leading to field emission across the Ag/ZnSe interface. The second mechanism is based on reports that a dominant compensating defect in p-ZnSe is Zn interstitials. From the free energies of formation, interfacial O will result in the formation of ZnO. Since interstitial diffusion is typically faster than vacancy diffusion, a significant fraction of the Zn used to form ZnO would be expected to come from Zn interstitials diffusing to the interface. This would reduce the number of compensating defects in the ZnSe, increase the net carrier concentration, and result in field emission across the Ag/ZnSe interface. These results have been summarized in a manuscript which was submitted to the Journal of Electronic Materials for publication.

Based on this hypothesis, the interfacial O would be present in the Ag/ZnSe contacts but not the Au/ZnSe contacts because O has a much higher permeation rate through Ag. As a result, attempts were made to increase the concentration of interfacial O in the Au/ZnSe contacts to see if a reduction in barrier height would occur. The Au was sputter deposited in 50% Ar and 50% O. Following deposition, the contacts were heat treated in an O ambient. These contacts were compared to Au/ZnSe contacts made previously by sputtering the Au in Ar and heat treating in forming gas (10% hydrogen, 90% nitrogen). The samples processed without O were found to have an as deposited barrier height of 10 to 15 volts, and no change in barrier height was observed for heat treatment temperatures of 150, 200, or 300°C. At heat treatment temperatures of 350 and 400°C, the barrier height dropped to a minimum of 3 to 4 volts. The samples sputtered and heat treated in O were found to have an as deposited barrier height of ⁻8.5 volts. This barrier height was found to drop to ⁻6 volts after heat treatments at 150 and 200°C, ⁻5 volts after heat treatment at 250 C, and a minimum of ⁻2.7 volts after heat treatment at 300°C. Heat treatment at 350° C was found to result in an increase in barrier height to 3 to 4 volts. SIMS analysis of the Au contacts indicated a significant increase in the O content for the samples sputtered and heat treated in oxygen. These results indicate that interfacial O may be useful in reducing the Schottky barrier height of metal/ZnSe contacts.

(b)   ZnTe Contacts

With respect to p-ZnTe, work has continued this quarter on a study of electrical contacts by Au films. Au (1500 Å) have been deposited by dc magnetron sputtering onto an MBE deposited overlayer of p-ZnTe (1100 Å) consisting of the Sony contact scheme for making ohmic contact to p-ZnSe (Fig. I.2). Annealing conditions to optimize the contact resistance to Au was determined from I-V data to be 200°C for 15 min. in forming gas. The I-V characteristics were slightly rectifying for as deposited contacts but became very ohmic upon annealing. The valence band offset was calculated to be 0.73 eV between Au and ZnTe, which should lead to a large tunneling current which provides the ohmic behavior of the contacts. AES depth profiles were collected from a sample annealed at 200°C for 90

minutes and no interfacial reaction products were detected. Work will continue to examine possible doping of the ZnTe by the Au contact.

(c)   GaN Contacts

Our investigation has continued of ohmic contacts to CVD grown, wurtzite n-type GaN (unintentionally doped $2x10^{18}$ cm^{-3}) using a Ti/Au (50 nm/200 nm)and Ti/Si/Au (10 nm/100 nm/200 nm) metallization schemes. Previously we reported that rapid thermal annealing (RTA) these contacts in a nitrogen atmosphere at 900°C resulted in linear I-V characteristics. Thermodynamic data indicates that TiN should form at the Ti/GaN interface during such anneals, and scanning Auger microscopy (SAM), secondary ion mass spectrometry (SIMS), and cross-section transmission electron microscopy (XTEM) were used to study this interface in Ti/Si/Au contacts. SIMS and SAM data are consistent with a TiN layer at the Ti/GaN interface. We are currently studying Ti/Si/Au contacts to MBE-grown, Si doped ($1.5x10^{20}$ cm^{-3} free electrons) GaN. In future work, Ti/Si/Au contacts will be evaluated on low free electron concentration ($1x10^{17}$ and $5x10^{17}$ cm^{-3}) n-type GaN, with a continued emphasis on minimizing contact resistance and maximizing the thermal stability of the contact with respect to temperature, time, and atmosphere. Additionally, an investigation of ohmic contact formation to p-type, MOCVD grown wurtzite GaN from APA Optics based on high melting temperature refractory metals or compounds will begin.

(III)   Microstructural Analysis of II-VI and III-V Materials (Kevin Jones)

(a)   Optical Degradation of Quantum Well II-VI Structure

A collaboration with 3M to investigate the degradation of II-VI laser diode structures has begun. Their early work indicated these laser structures fail in a similar fashion for both optical and electrical degradation. Because of the control afforded, optical degradation will be the initial focus for degradation. A multi-layer structure consisting of a ZnCdSe quantum well confined by two n-type ZnMgSSe layers, lattice matched to GaAs, has been degraded optically with the 350 nm wavelength laser at the power density of 140 W/cm^2. Cross-sectional transmission electron microscopy (XTEM) samples were prepared from both the non-degraded and degraded material. Analysis of the non-degraded material showed very few if any extended defects. XTEM analysis of the optically degraded material showed the presence of half loop. Most of these dislocations appear to extend down from the surface through the upper ZnMgSSe layer and the ZnCdSe quantum well but not all the way to the ZnMgSSe/GaAs interface. These dislocations however appear to extend only 0.1 microns below the quantum well into the 0.7 microns thick ZnMgSSe layer. Other regions showed dark contrast areas bound by half loops which appear to be the same defects discussed above but viewed from an orthogonal direction. Further examination of the evolution of these defects due to laser irradiation is in progress.

For the study of optical degradation of II-VI lasers, the 3M company has agreed to supply samples. Four different structures consisting of ZnSSe cladding layers (n-type on n-type) with ZnCdSe single quantum well, grown by MBE have been received. In these layers, the sulfur content has been varied slightly which results in different threading

dislocation densities from 1×10^6 cm^2 to 1×10^8 cm^2. These samples will allow us to study the influence of the initial defect density on the degradation process. These samples will be degraded using an excimer laser in Dr. Simmon's group at UF. The change in strain in the structure and microstructural defects due to optical degradation will be investigated using TEM, HRXRD and Raman spectroscopy (Dr. Holloway's group). Any change in the femtosecond free carrier lifetime will be studied as a function of degradation by Dr. Simmon's student and correlated with our microstructural studies.

A second study will focus on electrical degradation using p-n junction material supplied by 3M. The equipment to monitor the degradation of II-VI LEDs has been assembled by Dr. Zory. II-VI LEDs will be fabricated in conjunction with Dr. Zory and the degradation defects generated during the light emission will be observed using an electroluminescence (EL) microscopy. XTEM and plan-view TEM analysis of the electrically degraded LEDs will be correlated with the EL microscopy observations and photodegraded material.

(b)   Structural Characterization of InN and InGaN Alloys

The study of InN and InGaN alloys was carried out because the InGaN alloys, with bandgaps varying from 2.2eV for InN to 3.2eV for GaN, have the potential to extend the operating wavelength of optoelectronic devices into the blue region of the visible spectrum. The research was focused on the growth and characterization of both wurtzitic and cubic materials.

Various ternary InGaN films having different compositions and binary InN films were deposited by metalorganic molecular beam epitaxy (MOMBE) on semi-insulating (100) GaAs at 500°C. Triethylgallium (TEG) and trimethylindium (TMI) were used as the gallium and indium sources, respectively. A nitrogen ECR plasma generated from N$_2$ gas was used as the nitrogen source. Electron microprobe analysis was used to determine the composition of the InGaN films. Cross-sectional transmission electron microscopy (XTEM) was used to evaluate the GaN microstructure.

The microprobe analysis (Fig. III.1) showed that there is a negative deviation from linearity in the indium incorporation i.e. the indium composition is lower than that predicted by the [TMI/(TMI+TEG)] ratio. This is because of a catalytic reaction caused by the presence of Ga atoms on the surface.

In order to determine whether cubic InN and InGaN was grown on the substrates, XRD studies of the films was carried out using a powder diffractometer. The x-ray scans showed that the cubic phase was present in all cases. Further analysis of the InN and InGaN layers by XTEM showed that the films were single crystal in nature. However, the layers were defective with stacking faults lying along the {111} planes appearing to be the major defect type. The defect density was lowest in the case of InN which also has the lowest mismatch with the GaAs substrate. Evaluation of these materials will continue.
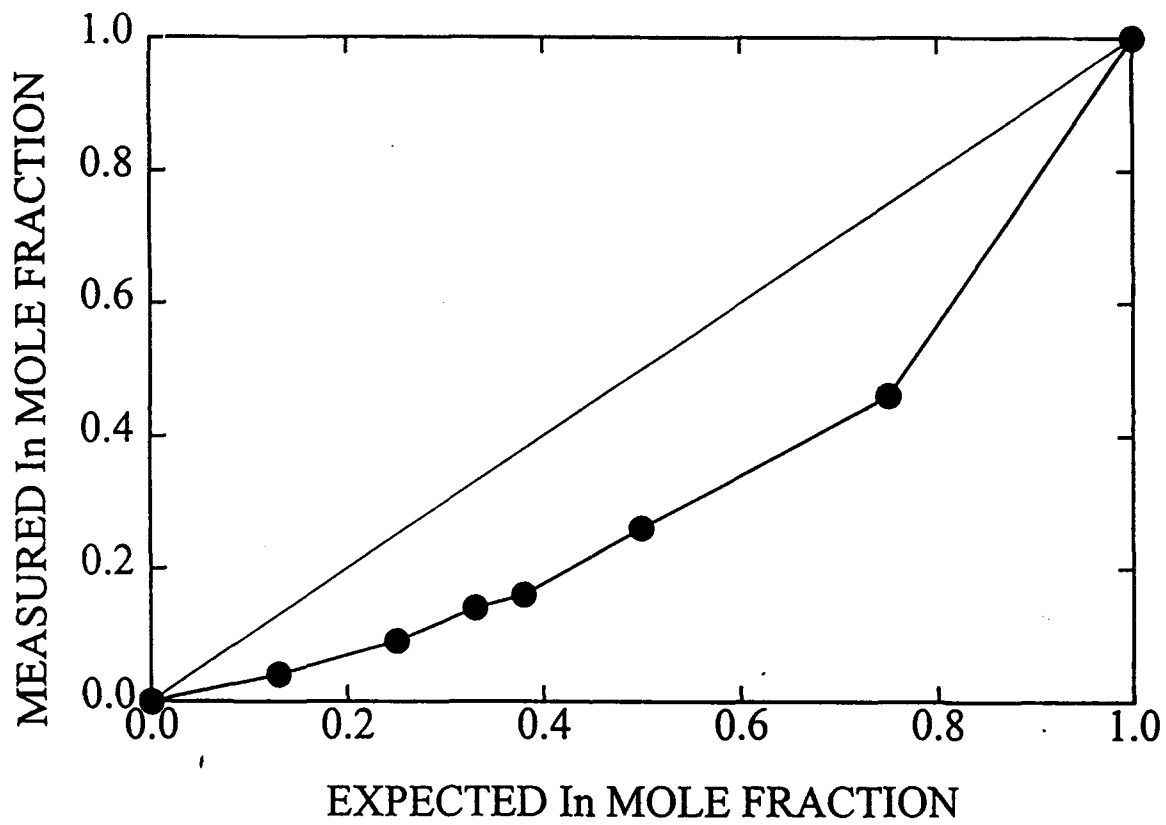
Fig. III.1: Relation between indium mole fraction of $In_xGa_{1-x}N$ i.e x and the flow rate ratio of indium to the sum of group III sources [TMI/(TMI+TEG)]

(IV)   Optical and Electrical Characterization of ZnSe   (J.H. Simmons)

Our research continues to focus on 3 tasks: (a) measurements of low temperature PL in support of the materials development effort, (b) measurements of time resolved PL measurements for a study of excited carrier dynamics in quantum well structures, and (c) a theoretical analysis of the carrier concentration and carrier mobility in doped semiconductors with the goal of understanding the role of various dopants in the formation of ionized defects.

(a)   PL measurements on novel materials

During the past quarter, we have conducted PL measurements and optical damage studies on a variety of ZnSe quantum well structures. The goals of such studies are two-fold: (a) to test damage resistance of various contact schemes, and (b) to monitor the lifetime of fabricated quantum well structures. Initial damage studies used exposure to a doubled, pulsed Ti-sapphire laser at 400 nm. Present studies use exposure to a pulsed nitrogen laser at 305 nm. The latter is less expensive to run and provides far more energy in longer pulses (600 ps). Damage formation in various quantum well structures deposited on ZnSe and GaAs substrates was studied in collaboration with Drs. Park and Jones as reported above. For example, ZnSe films deposited on a ZnSe single crystal substrate show a PL intensity decay after about 12 hours, while those deposited on GaAs substrates show a similar decay in intensity after about 2.5 hours. Damage studies of 3M samples are currently under way. In these samples, we plan to study optical and electrical damage to quantum well structures by analyzing the decay in free carrier lifetimes and by high resolution electron microscopy.

(b)   Time resolved PL studies

Time resolved studies of free carrier lifetimes are being successfully conducted. We have examined the free carrier lifetimes of ZnSe/ZnCdSe quantum well structures, provided by Dr. Park. An example of a typical measurement is shown in Fig. IV.1. The top graph shows the decay of the photoluminescence intensity at room temperature, while the bottom curve shows the logarithmic intensity. It is clear that only 1 decay process is present and its characteristic time varies between 300 and 400 ps depending on the sample growth temperature during MBE growth. The higher growth temperature gives the longer lifetime.

(c)   Analytical modeling of the carrier concentration and mobility in doped ZnSe films

A numerical approach for calculating the full solution to the Boltzman Equation was modified to apply to ZnSe. This approach calculates the full carrier and impurity screening contributions, generally ignored by other investigators, which are, however, essential at high dopant concentrations. Full calculations were conducted both numerically and in closed form for the carrier concentration and mobility dependence on temperature and doping level. These studies have revealed a semiconductor-metal transition when the hopping density approaches the inverse of the cube of the defect center Bohr radius.

PECS SPECTRA OF ZnCd MQW 50/50 ROOM T
under 400nm 140fs pulse excitation
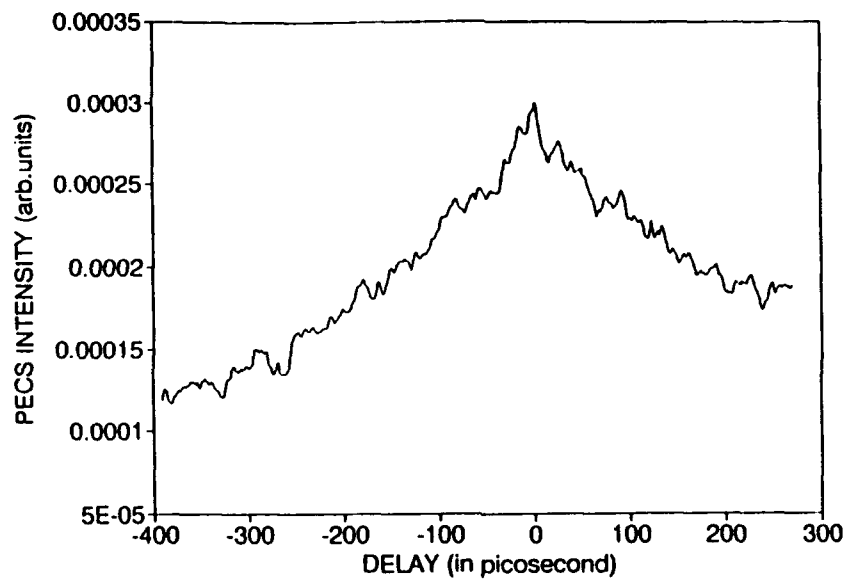
PECS SPECTRA OF ZnCd MQW 50/50 ROOM T
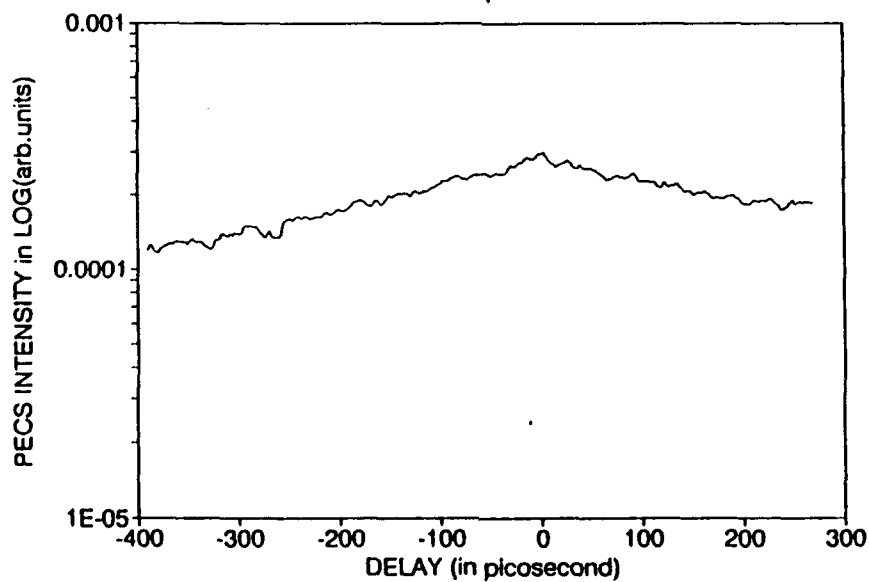### under 400nm 140fs pulse excitation

Fig. IV.1

The modeling work has given us insight into the nature of the semiconductor-metal transition which is observed in heavily doped films. Our approach seems to have uncovered a new way of examining such transitions. We are currently studying its implications. Two papers are in preparation.

(d)   Plans for next quarter

We plan to conduct PL measurements on GaN films, and quaternary and ternary films from the system ZnMgSeS. This will require detection at shorter wavelengths which can be achieved with our present equipment. Research on the effects of optical radiation and diode current operation on free carrier decay times and structural defects will continue. Time resolved PL studies will be applied to understanding the effect of point and/or extended defect growth on the trapping and recombination processes which affect free carrier lifetimes. The plan is to develop a relationship between structural defect formation and carrier lifetimes and identify the mechanism by which lasers and photodiodes degrade with use. Modeling studies are under way for p-doped semiconductors in order to compare the self-compensation effects with those in n-doped ZnSe semiconductors.

(V)   MOCVD Growth of MgZnCdS Thin Films (Tim Anderson)

(a)   MgZnCdS Films

The goal of this research is to explore the feasibility of the new pseudoternary material system $Mg_xZn_yCd_{1-x-y}S$ for the fabrication of visible light emitters. The motivations for examining this system include the possibility of lattice matching to GaAs, wide range of bandgap energies, and avoidance of Se. Work to date has focused on the ternary limit $Zn_xCd_{1-x}S$, although some work on the deposition of $Zn_xMg_{1-x}S$ has been performed. The $Zn_xCd_{1-x}S$ films have shown a large stacking fault density and a parametric study has been conducted to minimize the defect density, as discussed below. As a result, we have identified growth conditions that have produced an order of magnitude lower FWHM of the (400) reflection rocking curves from the (400) diffraction peak as compared to our initial films. This value, 500 arc sec, is the lowest reported in the literature for this growth chemistry.

As mentioned in the previous report, a study was initiated to determine the correlation of the FWHM from HRXRD with growth temperature for the five following substrate orientations: (111)B, (111)A, (100) 5° toward the nearest <110>, (100) 2° toward the nearest <110>, and (100) 0° toward the <110>. Figure V.1 shows a clear downward trend of the FWHM with increasing growth temperature. The quality of the films grown on the (111) substrates are substantially better than for (100) substrates. Films were not grown at temperatures greater than 550°C because net growth did not occur due to the high decomposition pressure of the films. At 600°C, there was no significant growth even with higher concentrations of reactants, i.e., the thermodynamic limit was reached at 600°C for reasonable values of the inlet reactant concentrations.

In Figure V.2, the FWHM is plotted against the VI/II ratio at a 300°C growth temperature. The results show a separation of two groups by their respective substrate

orientations. The (100) substrates show poorer crystal quality than the (111) substrates, with the quality improving with decreasing VI/II ratio. The results seem to merge at a VI/II value of around 15-20 where lack of S is likely causing point defects that produce degradation of the crystallinity for (111) orientations. After a growth plane of II atoms are deposited on (111) planes, more S is needed for the next plane to continue the growth. Growth on (100) substrates requires II atoms and S simultaneously. Growth on (111) planes acts inherently like atomic layer epitaxy because of the attraction and repulsion of cations and anions for a particularly charged growth surface.

One way to improve crystallinity of ZnCdS is to grow a buffer layer prior to the growth of ZnCdS. This has been shown to be effective for many binary and ternary III-V system. Exploring this idea, a buffer layer of ZnSe was grown prior to ZnCdS and the results are shown in Figure V.3. The plotting symbols represent the same ones as in Figure V.2. The growth temperature of ZnCdS was held constant at 550°C while the ZnSe buffer layer was grown either at 350 or 550°C. The results again clearly depend on the substrate orientation. For the (111) substrates, the addition of a buffer layer does not seem to have any significant effect while that for the (100) substrates seem to degrade the crystallinity tremendously. Thus a ZnSe buffer layer does not significantly improve the crystallinity of ZnCdS. The real mechanism by which a buffer layer improve crystallinity is still not clear. One possibility is that a buffer layer creates an extremely clean surface for growth. With that in mind, a ZnSe buffer layer was grown and then subsequently ramped to higher temperatures while still maintaining the correct S overpressure to eliminate revaporization of the grown material. The temperature was increased to 650°C and then reduced to a growth temperature of 550°C. Again the results showed no improvements with worse results than simply growing the buffer layer at the cited two temperatures.

The role of the etchant in substrate preparation on the quality of the ZnCdS film was also investigated. As shown in Figure V.4, three etching procedures were used in the normal cleaning process prior to growth. Etching in a $NH_4OH:H_2O_2:H_2O$ (20:7:100) solution for 5 min gave the best results, regardless of the substrate orientation.

We have also performed initial doping studies and the films are being characterized. We have installed a new S precursor, methyl mercaptan, based on a communication that this precursor greatly reduces the staking fault density.

(b) GaN Thin Films

The short term objective of our approach to improve the quality of GaN-based films is to take advantage of known catalysts for the thermal decomposition of NH_3. The basic idea is to pattern these known catalysts (e.g., W, Mo, TiC) on sapphire substrates and perform selective area epitaxy. These catalysts would hopefully produce a greater concentration of atomic N radicals at a lower temperature, thus providing improved film stoichiometry. This effort has begun with a program to identify the optimal growth conditions on unpatterned substrates. In particular, two factors have been identified that result in improved surface morphology and film structural quality. One of these factors is the length of initial surface nitridation and the other is the use of a two-temperature step growth process.

X-ray diffraction spectra of GaN films grown on $Al_2O_3(0001)$ and 6H-SiC(0001) substrates obtained under identical growth conditions are shown in Figures V.5 and V.6,
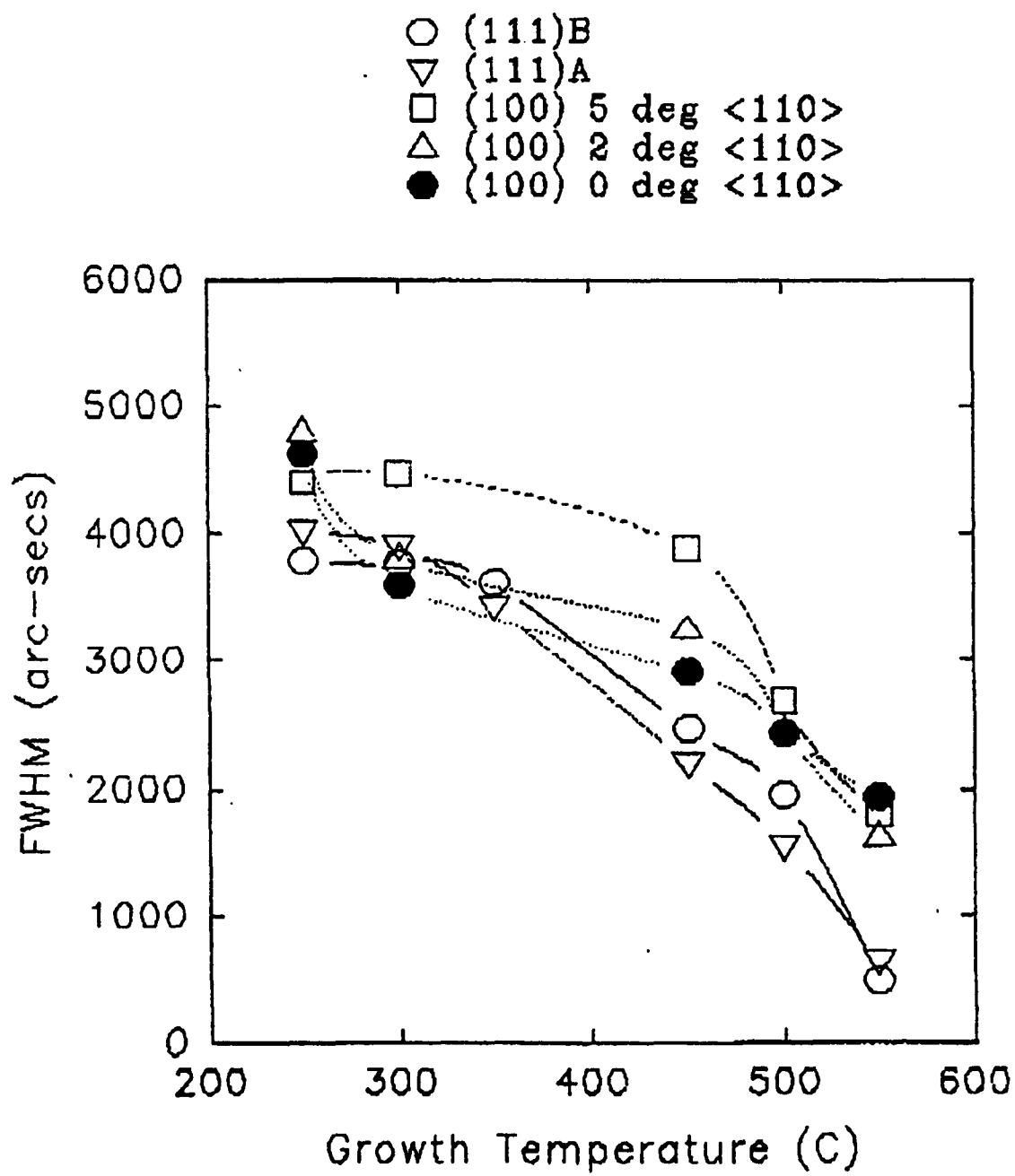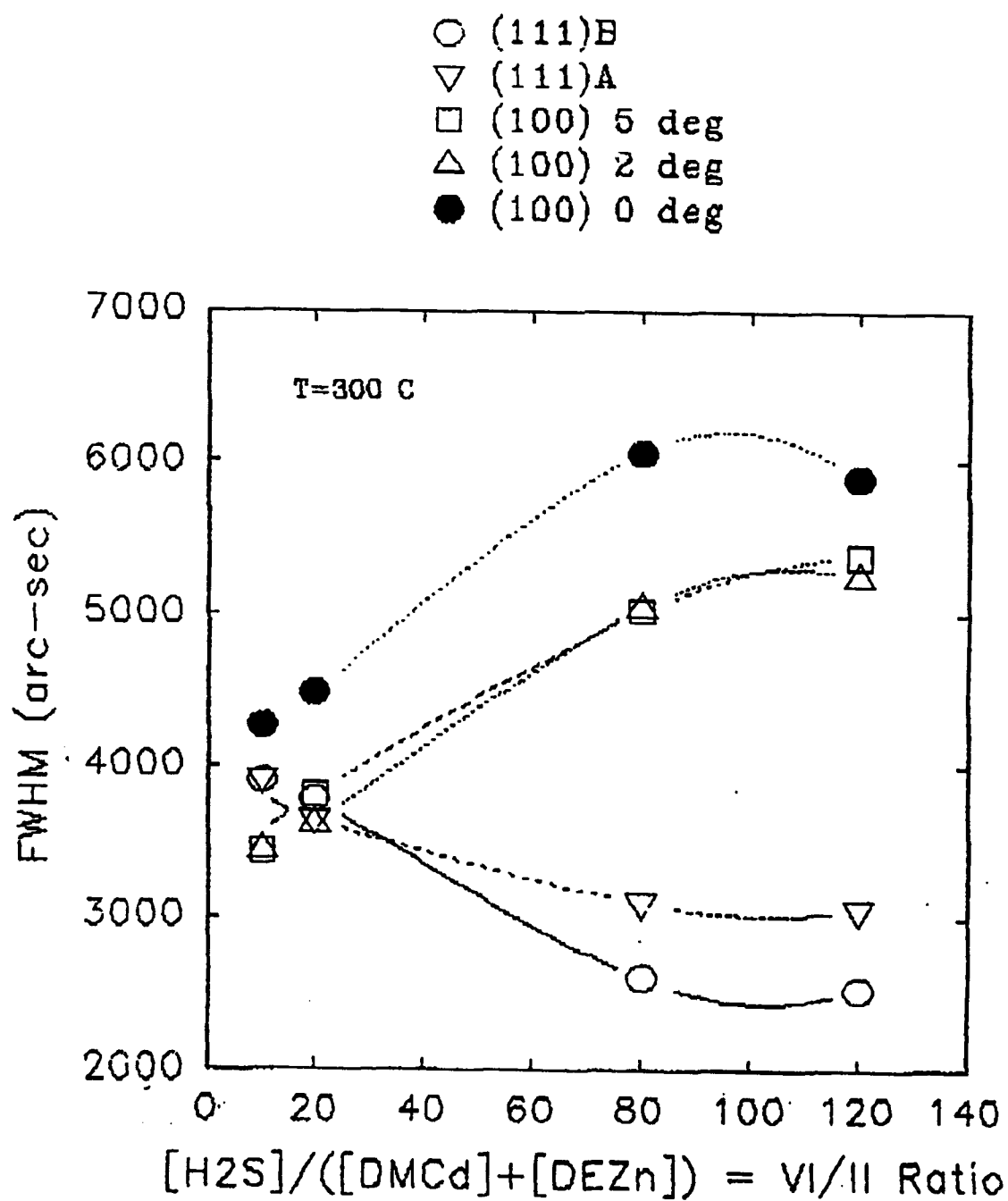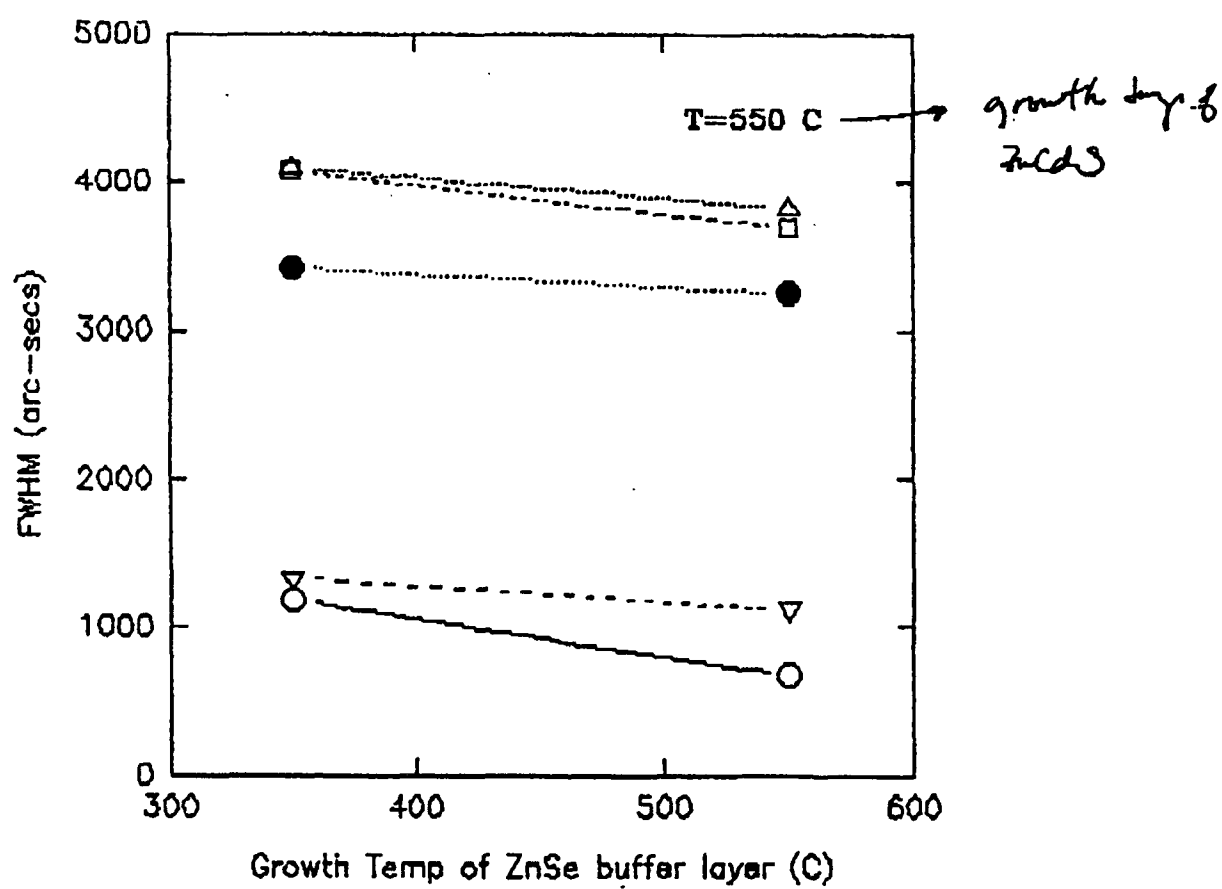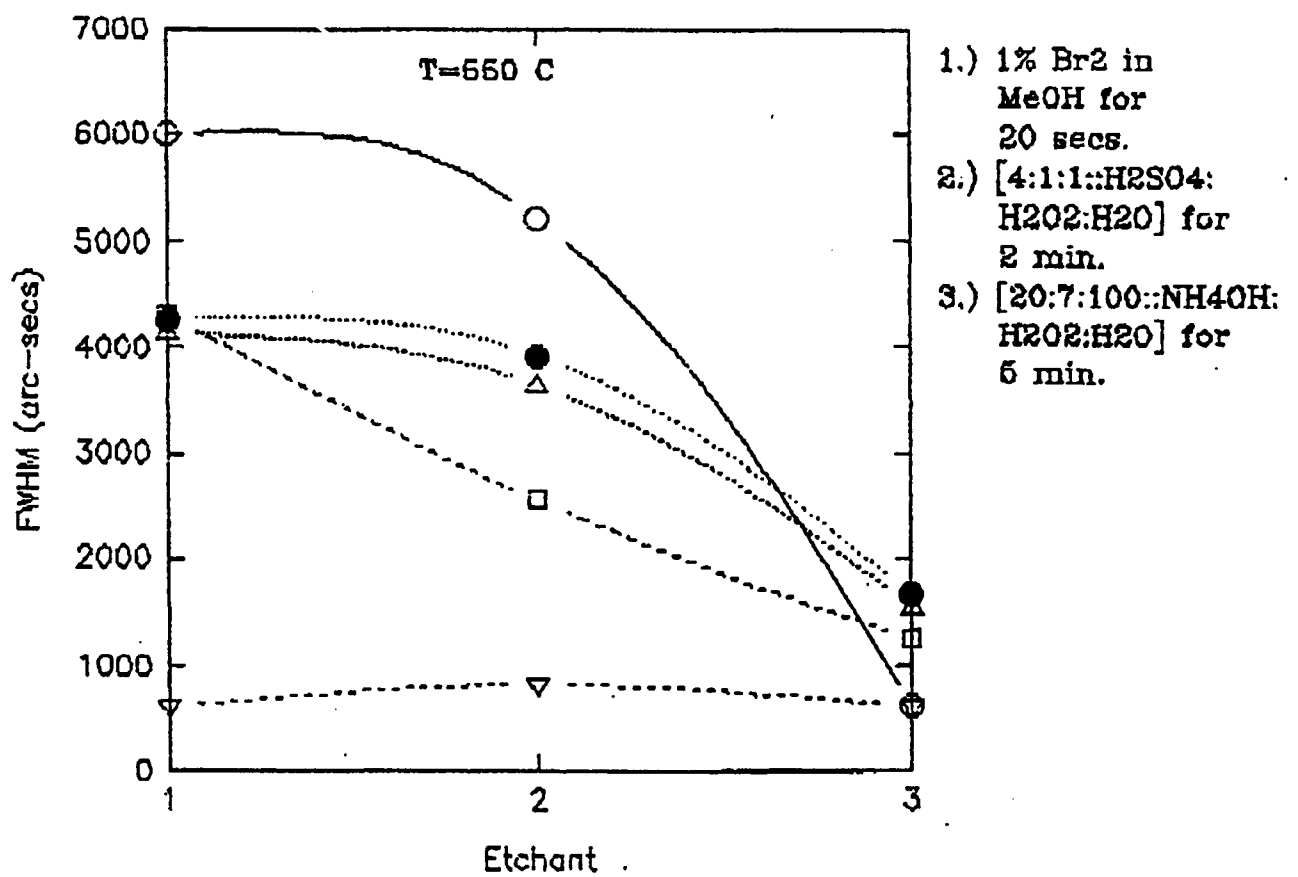
Fig. V.1.

Fig. V.2.

Fig. V.3.

Fig. V.4.

respectively. In Figure V.5, the two peaks correspond to the same hexagonal peak signifying the first order and second order peaks at 34.88°(0002) and 73.08°(0004), respectively. Since there is only one strong peak, the film can be termed as epitaxial. The crystal structure obtained on 6H-SiC in Figure V.6 also indicated epitaxy due to the presence of a single peak at 34.76°(0002); the other adjacent peak at 35.75° is due to (0021) peak originating from the underlying SiC substrate.

The optical properties of the above films were also evaluated by PL measurements as shown in Figure V.7 and V.8. The excitation source used was a 10 mW He-Cd laser. A strong room temperature PL peak at 3.39 eV was obtained from both films. The surface morphology of GaN film obtained on the 6H-SiC surface was observed to be smoother than produced on the Al_2O_3 surface. The 0.5 μm films on both substrates are specular and free of pin holes. Since the growth of epitaxial films on unpatterned substrates has been demonstrated, our efforts will now focus on 'selective' area growth of GaN.

(VI) Development of Diode Lasers (Peter Zory)

(a) Diode Pumping

Stripe geometry type devices with cleaved facets were fabricated from CdZnSe/ZnSe multiquantum well material grown by MBE in Dr. Park's laboratory. The temporal dependence of light emission versus drive current as well as spectral behavior were measured. Although output power levels close to 1 mW per facet were measured at 85 K, spectral narrowing due to gain was not observed.

(b) Degradation Studies

New photolithography masks were utilized to fabricate thin gold contact LED devices on CdZnSe/ZnSe quantum well material provided by 3M. An apparatus was built which allows us to observe (using a TV monitor) how defects grow in the material as a function of time and drive current. The first wafer we have studied degrades by the growth of what appear to be point defects into larger point defects, characteristic of material with defect densities greater than 10^8 cm^2. We plan next to process some 3M material with defect densities of about 10^6 cm^2 with the goal of generating dark line defects (DLDs). Dr. Guha of 3M believes that DLDs in ZnSe-based materials are not due to the formation of dislocations, contrary to the fact that DLDs in GaAs-based materials are believed to be due to dislocations.

(VII) Theoretical Calculations of Dopants of ZnSe (Gertrude Neumark)

As mentioned previously, work in the literature has reported a change with temperature in the activation energy of the N acceptor, and explained this by assuming the N acceptor to be located interstitially. An interstitial location implies high ion mobility, which is cause for concern. We therefore decided to check whether the change in activation energy can be explained by a temperature dependent screening, since screening is known

XRD Spectrum of GaN Film Grown on Al$_2$O$_3$(0001)
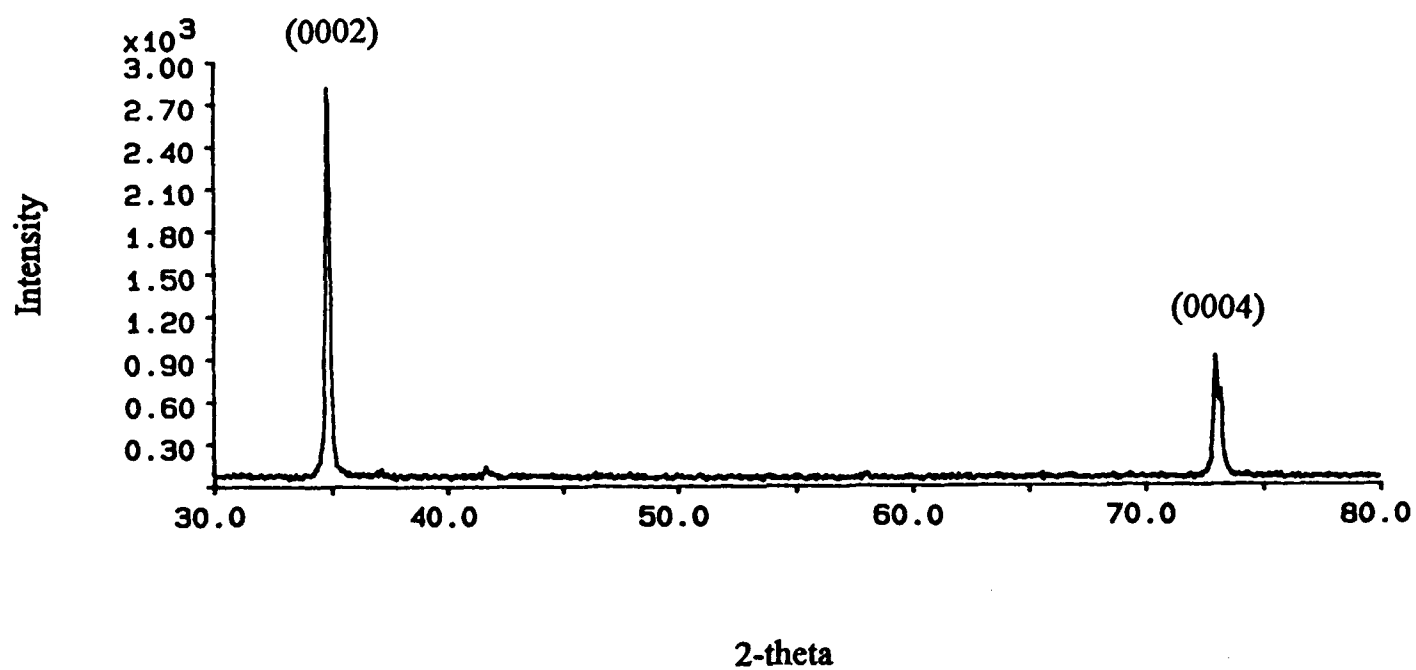

Fig. V.5.

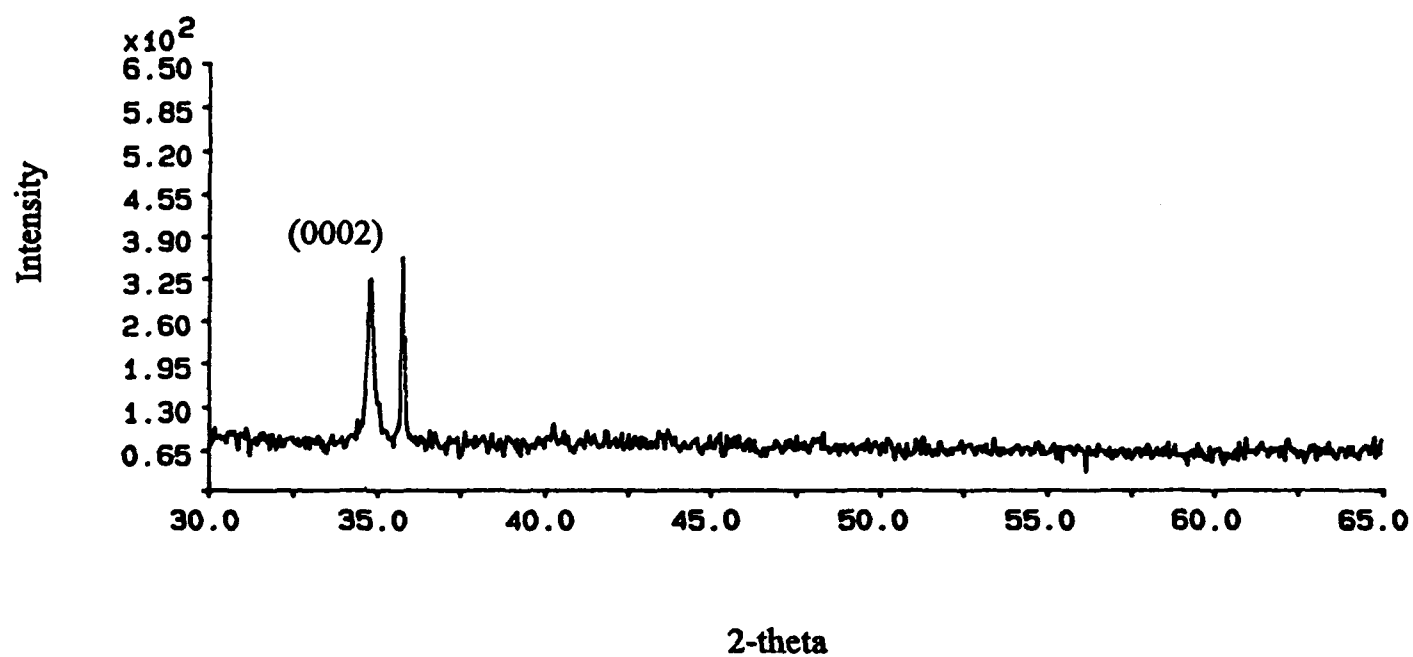# XRD Spectrum of GaN Film Grown on 6H-SiC(0001)

Fig. V.6.

Room Temperature PL Spectrum of GaN grown on 6H-SiC(0001)
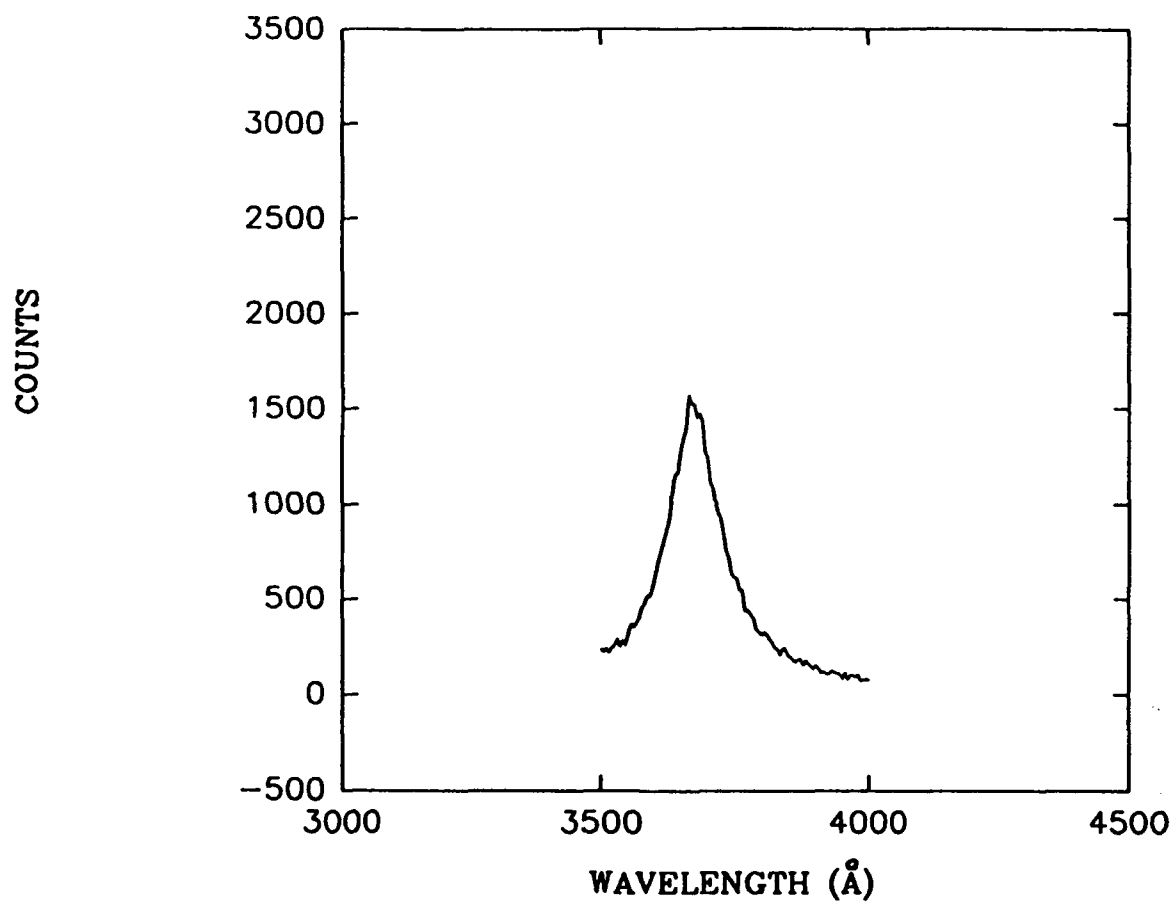

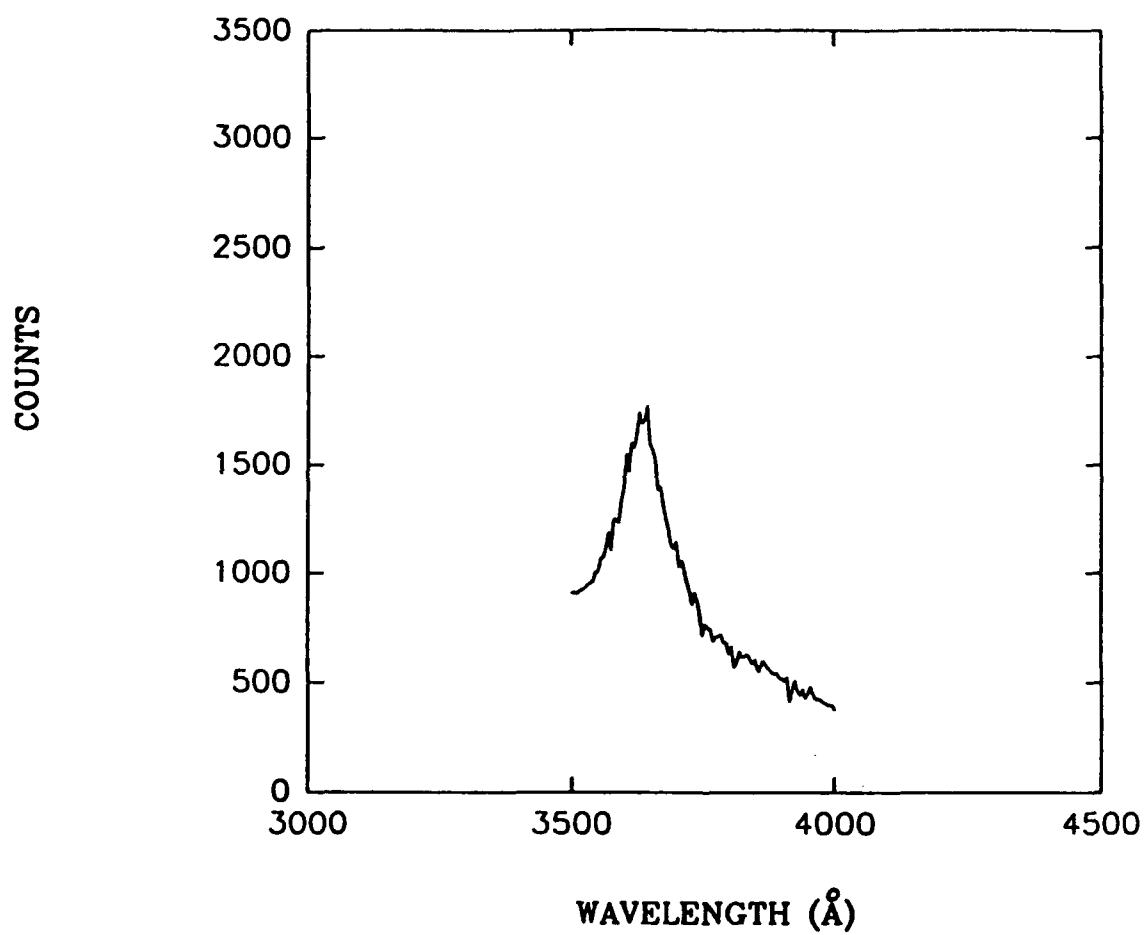Fig. V.7.

Room Temperature PL Spectrum of GaN Film Grown on Al$_2$O$_3$(0001)

Fig. V.8.

to cause a change in activation energy [Neumark, Phys. Rev. B $\underline{5}$, 408 (1972)]. If screening is the cause, there is no need to invoke an interstitial location.

We found that screening, with reasonable parameter values, could account for the results over a good part of the temperature range (up to about 180 K). At the higher temperatures, complications arise due to the possibility of transitions to an excited acceptor state. In addition, the luminescence peak which was used to obtain the experimental value was a relatively small shoulder on a different peak, and we question whether its location can be sufficiently well determined for meaningful comparison with the theory.

We then investigated the question of preferential pairing (which as mentioned in the previous report, is indicative of a <u>high</u> ion mobility) for the deeper donor known (from the literature) to be introduced into ZnSe at high N concentrations. This conclusion is based on observation of a donor-acceptor pair luminescence peak. Specifically, we are calculating the shift in peak position with excitation intensity to see whether values reported in the literature can be explained without preferential pairing, or whether such pairing is required to explain the results. [It is known that preferential pairing gives a stronger peak shift - Radomsky, Yi, and Neumark, J. Cryst. Growth $\underline{138}$, 99 (1994)]. We found that for a Bohr radius of 30 Å and an acceptor concentration of 10^{16} to $10^{17}/cm^3$, preferential pairing <u>is</u> required to explain that data of Zhu et al., [Appl. Phys. Lett. $\underline{64}$, 91 (1884)]. We will however still have to investigate further parameter ranges to better establish this conclusion.

(VIII) MOCVD Growth of GaN (Jacques Pankove)

Our objective is to grow p-n junctions in GaN that will be the basis for short wavelength emitters and lasers. In the past quarter, much of our effort has been directed towards careful characterization of our Mg-doped films. The intentionally doped films, while quite insulating, showed no luminescence at room temperature. When examining a subsequent run in which Cp_2Mg was not intentionally introduced, Mg-related luminescence lines were observed. Figure VIII.1 shows the 6K cathodoluminescence of such a film. The highest energy (3.27) eV peak has been extensively reported in the literature [1] and has been attributed to D-A radiative transition between an unidentified donor level and a Mg-related acceptor. The lower energy peaks are believed to be LO phonon replicas. Figure VIII.1 also shows a gaussian peak fit for these four lines. This data suggests that the high concentration of Mg incorporated in the intentionally doped films is somehow quenching the luminescence, and that a lower Mg concentration is necessary.

Room temperature photoconductivity spectroscopy was also utilized to help identify defect and impurity states in our doped and undoped films. Figure VIII.2 shows typical spectra of doped (214, Akasaki) and "undoped" (511) samples. All of the samples studied showed an exponential Urbach tail over several orders of magnitude, from the near infrared to near ultraviolet. The high quality undoped film, however, showed an additional steeper region near the band gap energy. This indicates the presence of states in the band gap. For laser diode applications, these gap states must be removed.

A modification of the gas delivery method of the first deposition system has produced very promising preliminary results. The system was modified such that the NH_3 and TEG are pre-mixed several centimeters from the heated sapphire substrate. In the few runs since the modification, the highest mobility for this system was achieved even without the use of
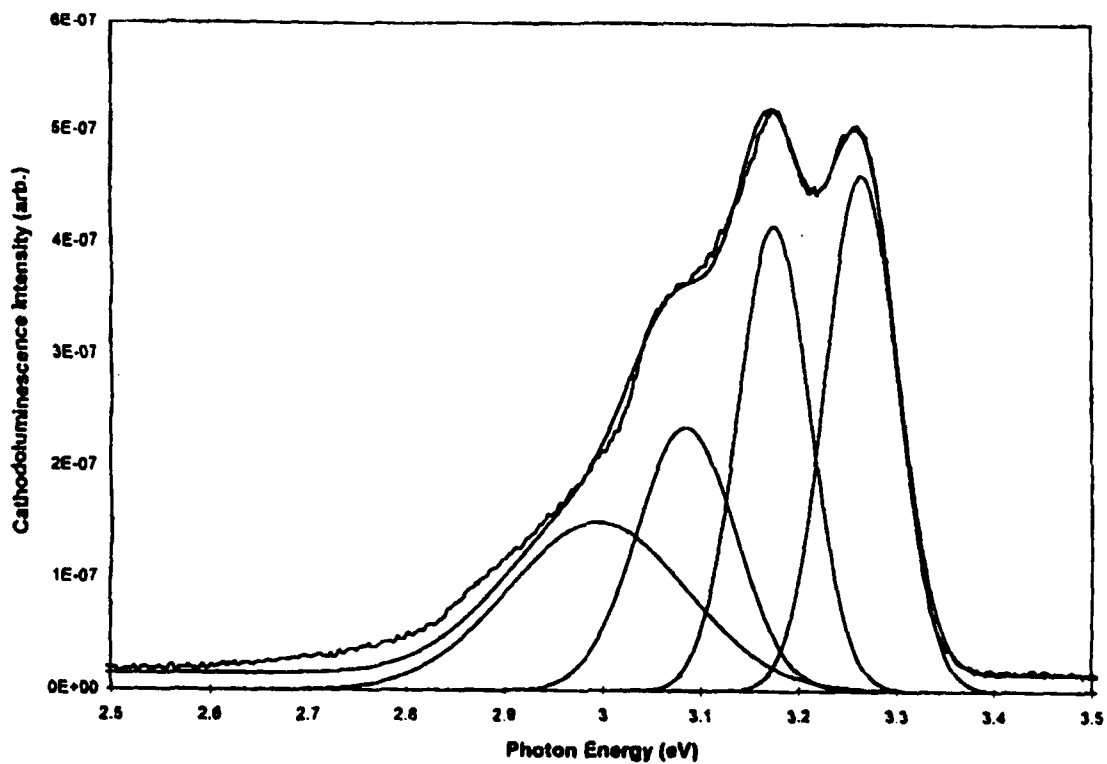
Figure VIII.1.   Cathodoluminescence spectrum of GaN:Mg (sample 225) at 6K and gaussian peak fit for 3.27eV D-A emission with three LO phonon replicas. The sum of the gaussian (smooth line) is plotted for comparison.
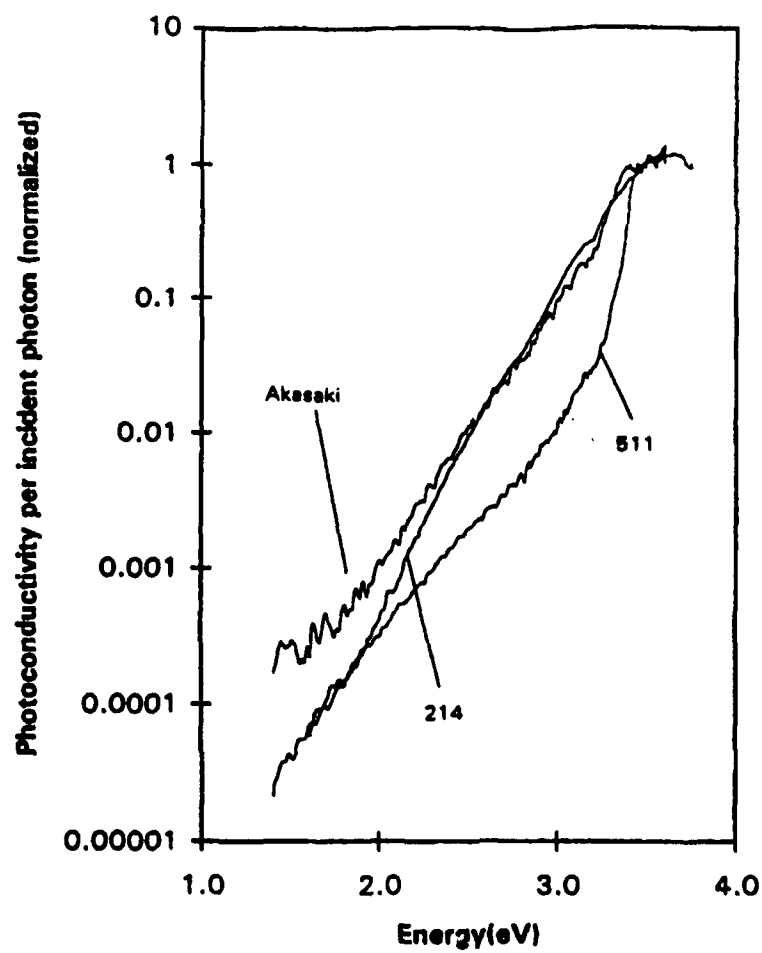
Figure VIII.2.   Photoconductivity spectra for Mg doped (214, Akasaki) and "undoped" (511) samples at 300K.

a GaN buffer layer. It is expected that further adjustments of growth conditions as well as the introduction of an optimized buffer layer will produce significant increases in crystal quality. In addition, a parallel project (SBIR funded) is in progress to produce single crystal GaN boules to provide GaN substrates. Homoepitaxial growth on GaN substrates should greatly increase the crystal quality of our films.

We recently installed a JEOL 35C scanning electron microscope which was donated to the University by the National Renewable Energy Laboratory in Golden, Colorado. This microscope will enhance our in-house film characterization capabilities.

(IX) Gain Modeling in II-VI Strained-Layer QW Structures (Reinhart Engelmann)

(a) Modeling of GaN Based Laser Structures

A review of the GaN state-of-the-art has been undertaken. Compared with II-VI lasers, less work has been reported on GaN based device models. Our efforts during this period was focused primarily on III-V nitride devices. Material data for modeling work were updated and collected from recent publications. Relatively speaking, there are much more data reported on nitrides of the wurtzite crystal phase than the zinc-blende phase. Although, in both cases, it is still insufficient to perform detailed gain calculation and modeling at this time, we can estimate basic device structures for the growth studies based on the general device properties that are available.

The band gap energy and lattice constant of both wurtzite and zinc-blende nitrides are plotted in Fig.1. SCH structures suitable for both diode laser and LED are available in each of the two phases, with GaInN as active layer, GaN as barrier layer and AlGaN as cladding. Both sapphire and ZnO (both are of hexagonal crystal structure) have proven to be suitable substrates for wurtzite GaN growth. 3C-SiC (cubic) and GaAs are used as substrates for growth of zinc-blende GaN.

Band-band transitions are desirable in the active layer for maximum efficiency. In view of the deep acceptor levels (about 0.5 eV above the valence band edge) which likely form an impurity band under the high doping condition necessary in the p-type cladding and barrier layers, the effective band gap of barrier and cladding could exhibit considerable shrinkage. Therefore the material band gap of these layers needs to be sufficiently higher than that of the active layer. This means that the concentration of In in the active layer has to be designed high enough (nearly 0.4 mole fraction) or, alternatively, the Al concentration in barrier and cladding needs to be increased.

(b) Doping Influence and Hole Freeze-out in II-VI Device Modeling

A model for carrier transport across the heterojunction and the metal-semiconductor interface has been studied for understanding the current-voltage characteristic in a ZnSe-based II-VI laser diode. For the heterojunction between cladding/barrier and active layer, we find that the continuity of the quasi-Fermi level across the interface should still be maintained in a QW laser, contrary to the suggestion by Horio and Yanai [2] who argued that quasi-Fermi levels need not to be continuous across the interface.

Fig. IX.1. Band gap vs. lattice constant of wurtzite (h-, basal
plane) and zinc-blende (c-) III-V nitrides. Dash-dotted
lines indicate lattice constants of common substrate
materials.
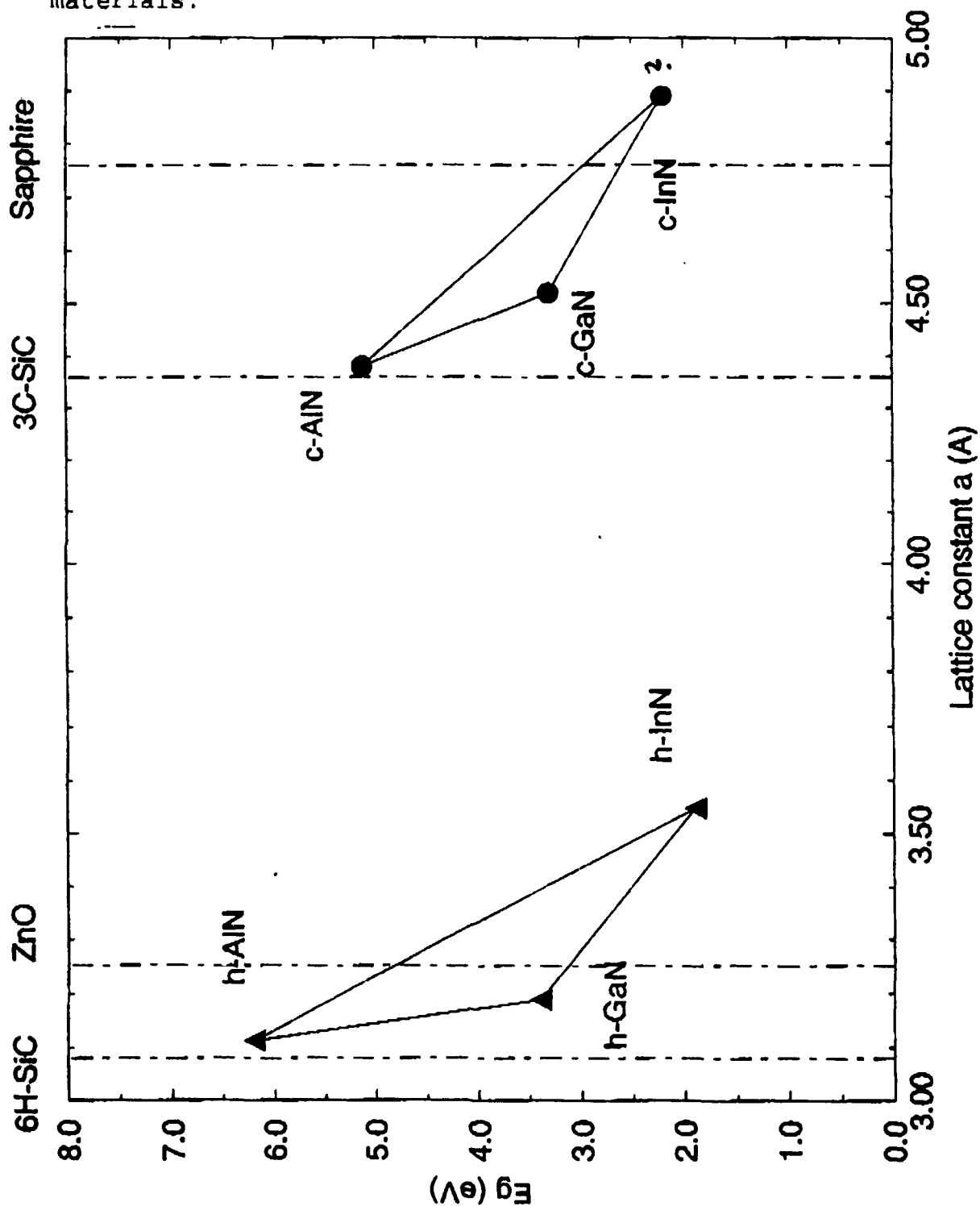
Considering the problem of hole freeze-out in II-VI devices, hole transport in the bulk p-type semiconductor can be explained either by the so-called Frenkel-Poole effect which assumes that the electric field is lowering the thermionic work function of a trapped carrier, or by the so-called impurity band conduction. The latter explanation may also be applied to the GaN based device. In addition, carrier injection from the metal contact needs to be considered which depends on the field distribution at the contact interface and in the p-type layer. By combining the p-type bulk transport model with the modeling of the interface between contact metal and p-type semiconductor (including the enhanced carrier injection into the semiconductor due to the presence of trapping centers), a full description of the I-V characteristic can be obtained. The programming work to incorporate the above phenomena is in progress.

(c)   Plans for next quarter

Upon further data collection on the nitrides, gain modeling will be performed and programming of the transport model will continue.

References

-     [1]   Amano, et. al., J. Electrochem. Soc., vol. 137, no. 5, 1639 (1990).
-     [2]   K. Horio and H.Yanai, IEEE Trans. Electron Devices, Vol. 37 (4), 1093 (1990)

Presentations this quarter

-     R. M. Park, "Molecular beam epitaxial growth of green light emitting diodes on ZnSe wafers," Electronic Materials Conference, Boulder, CO, June 22-24, 1994.

-     R. M. Park, "High mobility zincblende GaN films grown by MBE," ARL Meeting on GaN and Related Materials for LEDs and LDs, CECOM Night Vision and Electro-Optics Directorate, Ft. Belvoir, VA, July 29, 1994--Invited.

-     P.H. Holloway and H. Arlinghaus, "Resonant Ionization Spectroscopy and Secondary Ion Mass Spectroscopy to Measure Trace and Dopant Level Elements in Semiconductors," Invited Lecture, 16th Annual Symp. on Applied Surface Analysis, Burlington, MA, June 15-17, 1994.

-     P.H. Holloway, "Surface and Materials Analysis: Synergism with Vacuum Technology," Invited Lecture, 1994 Annual Symp. of the New England Chapter of the AVS, Burlington, MA, June 14, 1994.

-     J. Fijol, J. Trexler, L. Calhoun, R. Park, and P.H. Holloway, "Ex-Situ Formation of HgSe Contacts to p-type ZnSe," 1994 Electronic Materials Conference, Boulder, CO, June 22-24, 1994.

Publications during quarter

- C. M. Rouleau and R. M. Park, "Real-time *in situ* monitoring of defect evolution at widegap II-VI/ GaAs heterointerfaces during epitaxial growth," Mat. Res. Soc. Symp. Proc. Vol. 324, 125 (1994).

- L. C. Calhoun, C. M. Rouleau, M. H. Jeon and R. M. Park, "p-Type ZnSe:N grown by MBE: evidence of non-radiative recombination centers in moderately to heavily doped material," J. Cryst. Growth, 138, 352 (1994).

- G. F. Neumark, R. M. Park and J. M. DePuydt, "Blue-green diode lasers," Physics Today, 47, 26 (1994).

- J. G. Kim, A. C. Frenkel, H. Liu and R. M. Park, "Growth by MBE and electrical characterization of Si-doped zincblende GaN films deposited on b-SiC coated (001)Si substrates," Appl. Phys. Lett. 65, 91 (1994).

- M. H. Jeon, L. C. Calhoun, and R. M. Park, "MBE growth of green LEDs on ZnSe wafers," accepted for publication in J. Elect. Mat.

- G.F. Neumark and G.-J. Yi, "II-VI Semiconductors: Crystal Defects," Encyclopedia of Advanced Materials, Vol. IV, p. 2383-2389 (Pergamon Press, 1994).

- R. Engelmann, "Advances in the state-of-the-art of GaN materials and light emitting devices", to be published in LEOS Newsletter.

Post Doctoral Associates, Graduate Research Assistants, and Undergraduate Research Assistants:

Post Doctoral Associates:

Chang H. Qiu with Dr. Pankove

Graduate Research Assistants:

Bruce Liu with Dr. Park
Austin Frenkel with Dr. Park
George Kim with Dr. Park
Jeff Hsu with Dr. Zory
Jason O. with Dr. Zory
Igor Kuskovskiy with Dr. Neumark
Li Wang with Dr. Simmons
Y. Cai with Dr. Engelmann
Charles Hoggatt with Dr. Pankove

Post Doctoral Associates, Graduate Research Assistants, and Undergraduate Research Assistants: (Continued)

Graduate Research Assistants: (Continued)

William A. Melton with Dr. Pankove
John Fijol with Dr. Holloway
T.J. Kim with Dr. Holloway
Jeff Trexler with Dr. Holloway
Steve Miller with Dr. Holloway
Eric Bretschneider with Dr. Anderson
Joe Cho with Dr. Anderson
J. Kim with Dr. Jones
S. Bharatan with Dr. Jones

Undergraduate Research Assistants:

Julie Sauer with Dr. Simmons
Greg Darby with Dr. Park
Bob Covington with Dr. Anderson
Michael Mui with Dr. Anderson
Brendon Cornwell with Dr. Anderson